A New Paradigm for the Extraction of Information : Application to Enhancement of Visual Information in a Medical Application

V. Courboulay[1]   A. Histace[2]   M. Ménard[1]   C. Cavaro-Ménard[2]

[1] Laboratoire L3i, Pôle Sciences et Technologie Université de La Rochelle, 17032 La Rochelle Cedex
[2] Laboratoire d'Ingénierie des Systèmes Automatisés, 62, avenue Notre Dame du Lac 49000 Angers,
vincent.courboulay@univ-lr.fr, histace@istia.univ-angers.fr,
michel.menard@univ-lr.fr, christine.menard@univ-angers.fr

Abstract

The noninvasive evaluation of the cardiac function presents a great interest for the diagnosis of cardiovascular diseases. Tagged cardiac MRI allows the measurement of anatomical and functional myocardial parameters. This protocol generates a dark grid which is deformed with the myocardium displacement on both Short-Axis (SA) and Long-Axis (LA) frames in a time sequence. Visual evaluation of the grid deformation allows the estimation of the displacement inside the myocardium. The work described in this paper aims to make robust and reliable the visual enhancement of the grid tags on cardiac MRI sequences, thanks to an informational formalism based on Extreme Physical Informational (EPI). This approach leads to the development of an original diffusion pre-processing allowing us to make better the robustness of the visual detection and the following of the grid of tags.

Keywords

Tagged MRI, PDE, anisotropic diffusion, Extreme Physical Information (EPI)

1 Introduction

The non invasive assessment of the cardiac function is of major interest for the diagnosis and the follow-up of cardiovascular pathologies. Whereas cardiac MRI only allows to measure anatomical and functional parameters of myocardium, tagged cardiac MRI makes it possible to evaluate the intra-myocardial displacement. Therefore, it allows the analysis of the regional contraction of the myocardium (detection of potential contractible areas within the infarcted area as it shown by [22]). The SPAMM (Space Modulation of Magnetization) acquisition protocol [30] used for the tagging of MRI data, displays a deformable $45°$-oriented dark grid which sticks to the contraction of myocardium (Fig.1) on the images of temporal Short-Axis (SA) and Long-Axis (LA) sequences. The 3D+T follow-up of this grid makes possible the evaluation of the intra-myocardial displacement and then could make easier the diagnosis of particular pathologies like ischemia for example.
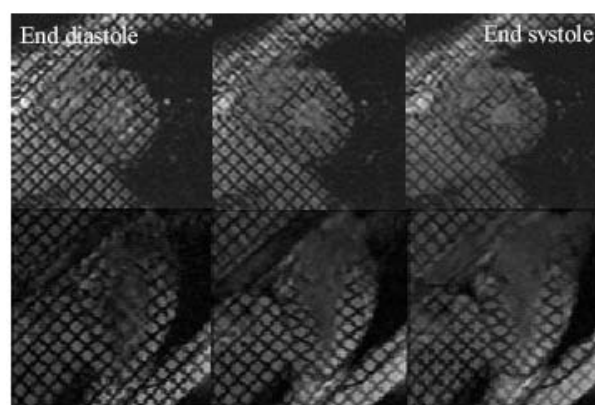

Figure 1: SA and LA tagged MRI of the Left Ventricle

Nevertheless, tagged cardiac images present particular characteristics which make difficult their processing. More particulary, images are of low contrast and their resolution is only of, approximately, one centimeter. Moreover they show complex deformations which are difficult to modelize and estimate, above all in case of pathological contractions of the heart. In [11], in order to solve these different problems, we presented a method for the detection and the follow-up of the grid of tags based on the use of a grid of active contours (B-snakes) for which a particular energy had to be minimized.

The clinical validation of the previous method made on 10 different sequences at the hospital of Angers, highlights three problems :

- Firstly, the method needs a precise estimation of the weight given to each energy of the grid of spline. Moreover, this estimation is different for each processed sequences.

- Secondly, the current model does not allow us to use this approach to detect and follow the grid of tags on LA sequences (the movement of the grid is no more a classical contraction).

- Finally, medical experts can only be ensured of the validity of the detected data by a visual appreciation of the results, which is for them insufficient. Indeed, the particular domain in which this method may be used (medical area), imposes the control of the potential error inserted by the scheme process of the tagged MRI, in order to ensure the clinical validity of the informations given to the medical expert and then, the validity of the final diagnosis.

These new problematic leads us to develop a scheme process more robust, more reliable in order to make better the reproducibility of the method, and adaptable to the detection on LA sequences. Moreover, it appears necessary to insert in this scheme a measure of the **uncertainty/inaccuracy compromise** for each step of the processing in order to ensure the validity of the detected information for medical experts. To do so, we propose to insert in the scheme process a restauration step based on an original informational formalism, recently developed in [8]. This variational formalism, elaborated in the area of the theory of measurement, appears to be totally adapted to the restauration of tagged MRI, and allows a better validity of the detected data as we will show it.

In this article, we present first this new restauration process and the underlying theory after having shown the insufficiency of usual methods of diffusion. In a second part, we present the application of the resulting diffusion process to our image processing problematic, and we follow with the presentation of results on *ad hoc* pattern, to follow with the obtention of a more precise and stronger energy image for the grid of active contours. At last, we present results of detection and following of the grids on tagged MRI with examples of exploitation of the extracted data.

2 Enhancement of visual information contained in tagged MRI based on an informational formalism

2.1 Isotropic and anisotropic diffusion

Image data restauration by diffusion equation is, by now, a well established approach [14, 28]. Classical diffusion schemes have been implemented on tagged cardiac images in order to enhance the "tag data". But, as it can be seen on figure (2) and (3), results are not satisfying at all.

As a matter of fact, it appears that classical restauration schemes are not well adapted to our problematic. Results we obtained, show the necessity of defining an original diffusion equation adapted to our special problematic *i.e.* tagged cardiac MR image restauration.

The following two subsections present a new diffusion scheme based on informational theory called Extreme Physical Information (EPI) recently developed by Frieden [8] and applied to image processing field by Courboulay and al [5].
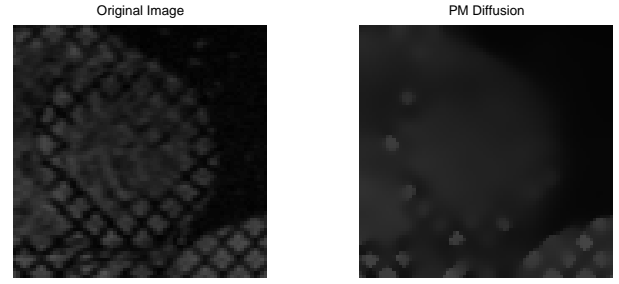

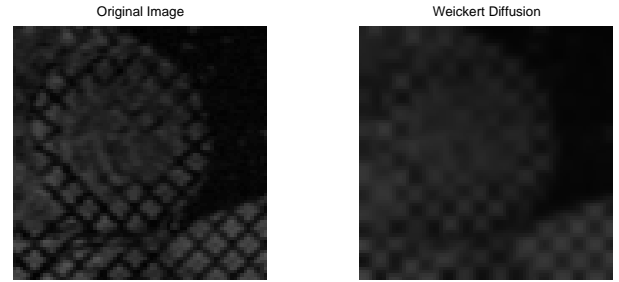Figure 2: Perona Malik Diffusion $dt = 0, 2$ 30 itérations

Figure 3: Weickert Diffusion $dt = 0, 2$ Iterations : 30

2.2 The extreme physical information principle

Let us consider a system under measurement. Then, we can represent the whole process of measure by the figure (4):
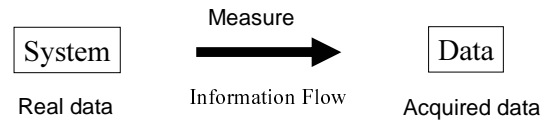

Figure 4: Informational Theory

As we can see, the acquired data are linked to the real ones through an information channel characterized by a transfer flow. The existence of this transfer gives rise to fluctuations on the acquired data compared to the real ones.

The unifying principle of physics, that of EPI, defined by Frieden [8] allows this kind of usual physical problems to be viewed within the following unified framework of measurement :

Considering the problem of estimating c vectors $v_i = (v_{i1}, v_{i2}, ..., v_{ip})$, $i = 1, .., c$, any fluctuations $y_i - v_i = x_i$ should occur with a probability

$$p_i(y_i/v_i) = p_i(x_i), \ x_i = y_i - v_i$$

Frieden shows that the accuracy in the estimates of the c parameters v_i is determined by the Fisher information I that has some useful physical properties [](*i.e.*, Fisher information may be regarded as a physical measure of

disorder which is related to experimentation). It provides new definitions of a variational approach finding a multiple-component probability density function law $p_i(x_i)$ of a vector variable x_i.

The Fisher information I in a multi-parameter, multi-component measurement scenario obeys [8] :

$$I[\mathbf{q}] = 4 \sum_i \int dx_i \sum_v \left(\frac{\partial q_i}{\partial x_{iv}} \right)^2 \qquad (1)$$

where

- $q_i \equiv q_i(x_i)$ is the ith component probability amplitude for the fluctuation $x_i = (x_{i1}, ..., x_{ip})$ in the measurement. They are the basic unknown items of the problem;

- $q_i^2(x_i) \equiv p_i(x_i)$ denotes the probability density function for the noise value x_i.

$I[\mathbf{q}]$ is called the *intrinsic* information, since it is a functional of the probability amplitudes that are intrinsic to the measured phenomenon.
Frieden defines a second information item called *Bound Fisher information* $J[\mathbf{q}]$ to embody all constraints that are imposed by the physical phenomenon under measurement. $J[\mathbf{q}]$ and $\mathbf{q}$ are generally found by applying the principle of *Extreme Physical Information*, which consists in optimising the physical information K of the system. K is defined by the following functional :

$$K[\mathbf{q}] = I[\mathbf{q}] - J[\mathbf{q}] = \text{extrem} \qquad (2)$$

Optimising K means optimising the loss of the perturbed Fisher information in its relay from the phenomenon to the intrinsic data (*i.e.* due to a measurement, the system is perturbed, causing a perturbation δJ in the bound information. The whole process of measure can then be modelled as it follows (cf. fig.(5)).
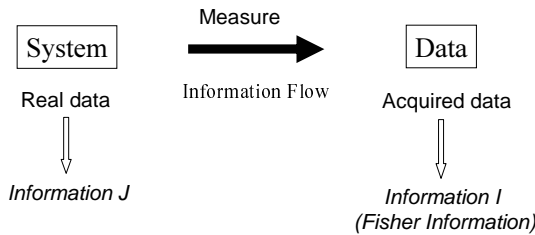

Figure 5: Fisher Information

Thus, it appears that such a theoretical area is totally well adapted to image diffusion in the way that it is important to ensure the validity of the enhanced data during the whole diffusion process (minimization of K). The following subsection presents the integration of the EPI axiomatic in the image diffusion process.

2.3 EPI and Image restauration

In order to integer the EPI axiomatic in the formulation of image diffusion, it is first necessary to identify each entity of our measuring process (cf. fig. 6). Courboulay and al. proposed in [5], to used the following parameters and the associated following errors in order to characterize the uncertainty/incertitude compromise :

- Spatial coordinates (x, y, z) are inaccurate due to the visual system acquisition process ;
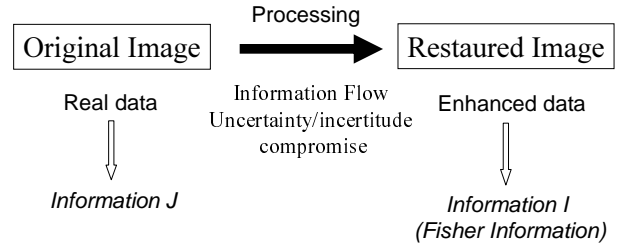
- Luminance values coordinates are uncertain ;

Figure 6: EPI and Image Diffusion

As a consequence, in order to minimize the loss of information during the diffusion process by controlling the uncertainty/inaccuracy compromise, the diffusion process must increase the certainty on the gray levels thanks to the local smoothing of the image. To take into account all these fluctuations (spatial, temporal, brightness) we define a four-dimensional vector $\mathbf{x} = (x, y, z, t)$ which leads to express two complex probability amplitudes characterizing these fluctuations (cf. Eq. 3).

$$\psi^* \psi = \frac{1}{2}(q_1 + iq_2) = p \qquad (3)$$

where q_i are the associated real probability amplitudes to ψ and p the amplitude probability.

In a simple space coordinates (*i.e.* $\mathbf{r} = (x, y, z)$, Fisher Information can be expressed in terms of ψ as follows (cf. Eq. (4)) :

$$I = 8 \int d\mathbf{r} \, (\nabla \psi)^* . \nabla \psi \qquad (4)$$

By taking into account the temporal fluctuations of $\mathbf{x}$, Eq. (4) becomes :

$$I = 8 \int \int d\mathbf{r} dt \times \left[(\nabla \psi)^* . \nabla \psi - \left(\frac{\partial \psi}{\partial t} \right)^* \frac{\partial \psi}{\partial t} \right] \qquad (5)$$

Thus, by expressing the uncertainty/inaccuracy compromise through the $\mathbf{x}$ vector, it is possible to obtain an expression of I to be used in a our given measurement scenario for EPI (diffusion). However, we also need an expression for the informational function J. In fact, since I is of a

fixed form (cf. Eq. (5)), the functional J uniquely determines the solution of the scenario.

In general, J follows from a statement of invariance about the system as we have seen before. Examples of invariance are :

- a unitary transformation, such as between direct- and momentum-space in quantum mechanics,

- the gauge invariance of classical electromagnetic theory or gravitational theory,

- an equation of continuity (invariance) of flow, usually involving the source.

Moreover, when the invariance principle is the statement of a unitary transformation between measurement space and a conjugate coordinate space then, functional J is simply the re-expression of I in the conjugate space [8].

For our application to MRI tagged restauration and more generally to image processing, this invariance property can be find through the Fourier Transform [5]. This unitary transformation between a measurement space and a conjugate coordinate space then allows us to express J as the re-expression of I in the Fourier area (cf. Eq. (6)) :

$$(\mathbf{r}, t) \overset{F.T.}{\leftrightarrow} (\mu/\hbar, E/\hbar) \tag{6}$$

Thus J is expressed as :

$$J = (8/\hbar^2) \int \int d\mathbf{r}dt \, \psi^*\psi \tag{7}$$

Once I and J defined, the physical information K of our given measurement scenario can then be defined as the difference between functionals I and J as seen before (cf. Eq. (8)).

$$
\begin{aligned}
K \quad &\equiv 8 \int \int d\mathbf{r}dt \\
&\times \quad \left[-(\nabla\psi)^*.\nabla\psi + \left(\frac{\partial\psi}{\partial t}\right)^* \left(\frac{\partial\psi}{\partial t}\right) - \frac{1}{\hbar^2}\psi^*\psi \right]
\end{aligned}
\tag{8}
$$

As a consequence, K is directly linked to the uncertainty/innacuracy compromise. The variational principle obtained by the extremisation of K must also verify this compromise, and by the way the diffusion process which represents in terms of image processing the previous principle obeys to the same compromise.

Using the Euler-Lagrange equation, the extremisation of K allows to obtain the corresponding diffusion equation.

$$\frac{\partial\psi}{\partial t} = \frac{\hbar}{2}\triangle\psi, \qquad \psi(\mathbf{r},0) = \psi_0 \tag{9}$$

This equation concerned the function ψ, nevertheless since ψ is closely related to the optimal convolution function, we can apply it directly to the image.

This equation, in image processing, can be interpreted as the one which allows the best results in terms of uncertainty/innacuracy compromise as we have seen before. This equation is the well known heat equation.

Nevertheless, such an equation can not be parameterized and then can not be adapted to particular applications. In the following section, we show how it is possible to extend this result to anisotropic diffusion.

2.4 From isotropic diffusion to anisotropic one

In order to extend these works to anisotropic diffusion, the following substitution of all derivatives in Eq. (8) can be found in [5] :

$$\nabla \to \nabla - \frac{\mathbf{A}}{\hbar} \tag{10}$$

$$\frac{\partial}{\partial t} \to \frac{\partial}{\partial t} + \frac{\phi}{\hbar} \tag{11}$$

Studies concerning invariance of gauge and anisotropic diffusion can be found in [23].

The integration of $\mathbf{A}$ and ϕ potentials, respectively vectorial and scalar, in our measurement scenario for EPI, allows the re-expression of the physical information $K = I - J$ (cf. Eq. (12)) as :

$$
\begin{aligned}
K \equiv 8 &\int \int d\mathbf{r}dt \\
\times &\left[-\left(\nabla + \frac{\mathbf{A}}{\hbar}\right)\psi^*.\left(\nabla - \frac{\mathbf{A}}{\hbar}\right)\psi \right. \\
&+ \left(\frac{\partial}{\partial t} - \frac{\phi}{\hbar}\right)\psi^* \left(\frac{\partial}{\partial t} + \frac{\phi}{\hbar}\right)\psi \\
&\left. - \frac{1}{\hbar^2}\psi^*\psi \right]
\end{aligned}
\tag{12}
$$

Extremisation of this re-expression of K leads to a new diffusion process given by :

$$\psi(\mathbf{r},0) = \psi_0$$
$$\frac{\partial\psi}{\partial t} = \frac{\hbar}{2}(\nabla - \mathbf{A}).(\nabla - \mathbf{A})\psi + \phi\,\psi \tag{13}$$

The $\mathbf{A}$ and ϕ potentials allow to rule the diffusion process and introduce some *a priori* about the image evolution. Usually, $\mathbf{A}$ acts on the spatial coordinates of the image, whereas ϕ is often taken to ensure the coherence of the results with the initial image. Concerning $\hbar$, if in quantic theory it is the Planck's constant, we can imagine to consider it as a function. This will be discussed at the end of the article.

By now, it appears that Eq. (13) can be adapted to different image problematics through a judicious choice for $\mathbf{A}$ and ϕ. Section (3) presents the particular parameterization we develop for the enhancement of the tag information in tagged cardiac MRI.

3 Application to the restauration of tagged cardiac MRI

3.1 Implementation of A

The choice of **A** is based on the particularity of the pattern to be enhanced in the tagged cardiac MR image, a $45\,^\circ$-oriented grid. As a consequence, the choice is based on the following constraints:

- smooth the non relevant information

- preserve the grid information

Then, we propose a choice for **A**, based on the fact that Eq. (13) allows a weighting of the diffusion through the difference between the local gradient and **A**.

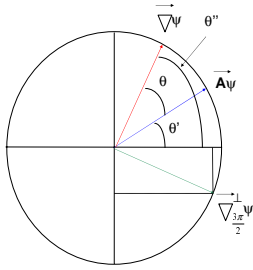To explain the way we implement **A**, let consider figure (7):

Figure 7: Local geometrical implementation of **A** in terms of the local gradient

The expression of the local gradient in terms of θ'' is :

$$\vec{\nabla}\psi = \left(\begin{array}{c} \|\nabla\psi\|\cos\theta'' \\ \|\nabla\psi\|\sin\theta'' \end{array} \right) \qquad (14)$$

and an expression of **A** in terms of θ' is :

$$\mathbf{A} = \left(\begin{array}{c} \|\nabla\psi\|\cos\theta' \\ \|\nabla\psi\|\sin\theta' \end{array} \right) \qquad (15)$$

As we can notice, we only impose the norm of **A**, in order to first make possible the comparaison with the gradient, and secondly not to restrict this choice to our application. As a consequence, the θ'orientation is not imposed at all.

Moreover, the most interesting expression of **A** would be the one expressing the vectorial potential in terms of θ, which represents the difference angle with the local gradient. If we made so, using trigonometrical properties and noticing that $\theta = |\theta'' - \theta'|$, we obtain a new original expression for **A** :

$$\mathbf{A} = \left(\begin{array}{c} \|\nabla\psi\|(\cos\theta''\cos\theta + \sin\theta''\sin\theta) \\ \|\nabla\psi\|(\sin\theta''\cos\theta - \cos\theta''\sin\theta) \end{array} \right) \qquad (16)$$

This expression (cf. Eq (16)) could be simplified by integrating the vectorial expression of the local gradient (cf. Eq. (14)) :

$$\mathbf{A} = \vec{\nabla}\psi.\cos\theta + \vec{\nabla}_{\frac{3\pi}{2}}^{\perp}\psi.\sin\theta \qquad (17)$$

At last, this result allows us to re-express Eq. (13) :

$$\frac{\partial\psi}{\partial t} = \hbar(\frac{\partial^2\psi}{\partial x^2}.(1-\cos\theta) + \frac{\partial^2\psi}{\partial y^2}.(1-\cos\theta)) + \phi\psi \quad (18)$$

This diffusion equation is an isotropic one, except in the case $\theta = 0$, where there is no diffusion process. Thus, a precise estimation of this angle can lead us to preserve particular patterns in the processed image. This is discussed in the following section for our application.

3.2 Estimation of θ

If the calculation of θ angle does not presents difficulties, the estimation of the relevance of its value is a more important criterium, and is directly linked to the local choice for the orientation of **A** (the norm being imposed).

The associated local orientation θ' of **A** is defined modulo π by using the inverse tangent [21] :

$$\theta' = \arctan(\frac{\nabla_y}{\nabla_x}) + \frac{\pi}{2} \qquad (19)$$

where ∇_y and ∇_x denote the components of the gradient vector on I_1 and I_2.

From now on, vectorial potential **A** is totally determined by its norm, direction and sens.

3.3 About ϕ

Concerning ϕ, as we have seen before, we are going to implement it as a potential of attraction to original data. This will allow the coherence of the final image at end of the diffusion scheme:

$$\phi = \lambda(I - I_0) \qquad (20)$$

As far as $\hbar$ is concerned, its influence has to be more precisely studied. However, because a choice is to be done, we propose to take $\hbar = 1$. The diffusion equation to be processed for the restauration of tagged MRI I can be re-expressed as follows in this case:

$$\frac{\partial I}{\partial t} = (1-\cos\theta).\frac{\partial^2 I}{\partial x^2} + (1-\cos\theta).\frac{\partial^2 I}{\partial y^2} + \lambda(I - I_0) \quad (21)$$

4 Results

4.1 Test of the diffusion process on *ad hoc* images

In this section, we present first, results obtained on simple images in order to show the restauration and denoising

potential of the method.

Let consider an image showing vertical, horizontal, and $45°$-oriented dark stripes on a uniform background. The diffusion process iterated 50 times for a step size $dt = 0, 2$, well shows the anisotropic effect of the Eq. (21) as we can see in figure (8).
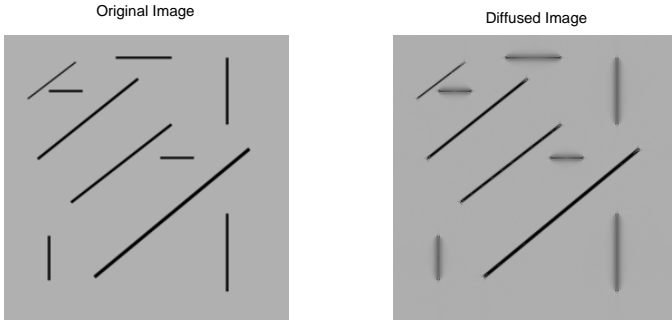

Figure 8: Diffusion on an *ad hoc* image

Imposing two possible orientations for **A** ($45°$, $325°$), it is possible to only diffuse data with not well oriented characteristic gradients. This property is characterized by the disappearing of the vertical and horizontal dark stripes in diffused image (cf. fig. (8)).

Moreover, if we apply this diffusion process to a noisy simple grid (cf. fig. (9)) imposing this time four possible orientation for **A**, it is then possible to show the denoising effect of the diffusion process.
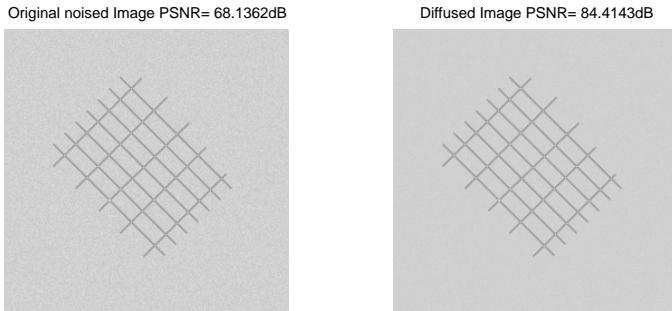

Figure 9: Diffusion on a perfect grid

Performing a zoom on the image, the result could be more appreciated :
As we intend to, the grid itself is not diffused at all and the increase of the Pic Signal to Noise Ratio (PSNR) from 68 dB to 84 dB, shows that the added gaussian noise is removed iteration after iteration.

4.2 Restauration of tagged cardiac MR images

The result gives in figure (11), shows the restauration of the $45°$-oriented tag on the first image of a tagged cardiac
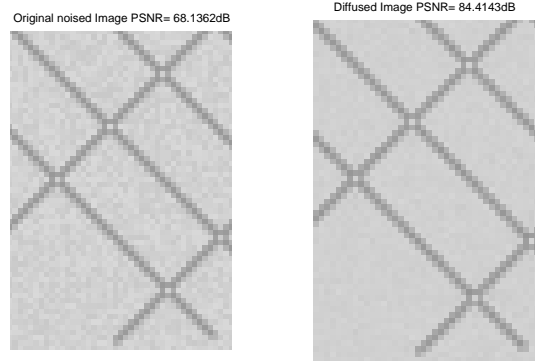

Figure 10: Diffusion on a perfect grid

sequence by the diffusion approach. The step size chose is 0,2. The iteration number is 60.
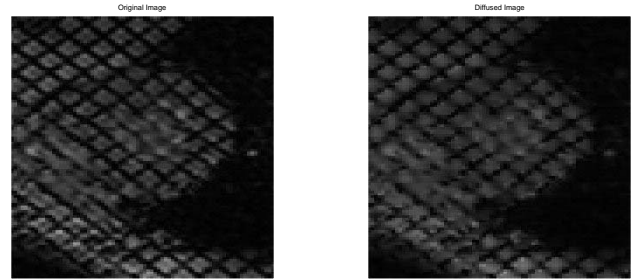

Figure 11: Restauration of tagged cardiac image

As we can see in figure (11), the diffusion process make possible the fading of noisy artifacts, and the non-$45°$-oriented lines. Zooming on a precise Region Of Interest (ROI) of the myocardium, it is possible to see the resulting anisotropic smoothing, particularly on the $135°$-oriented tags (cf. fig. (12)): they are disappearing.
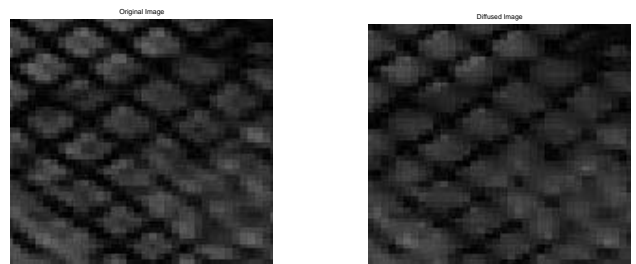

Figure 12: Restauration of tagged cardiac image

Moreover, because the orientation of **A** is locally calculated taking into account a particular neighborhood, is also possible to see that even if the tag is locally deformed due to myocardial contraction, the diffusion process remains efficient.

5 Discussion and outlines

The method presented in this article and based on both active contours and diffusion process issued from an infor-

mational approach, finally allows to:

- smooth the image with a preservation of the tag patterns

- increase the quality of the original image by its denoising effect,

- maximize the information transfer during the diffusion process in order to be sure of the validity of the enhanced data,

- ensure a stable and reproducible processing of the tagged cardiac MR sequences.

The method has to be validate on a larger number of patients. A protocol of that kind has been begun at the CHU of Angers working on a representative population of healthy and non-healthy patients.

Coupling the detection method of the grid of tags with an original automatic detection of the myocardial boundaries (epical and endocardial ones) based on the use of active contour and texture analysis [12], it is possible to realize a 2D+T map characterizing the local deformations of the myocardium (cf. fig. (13)).

1st – 2nd   2nd – 3rd
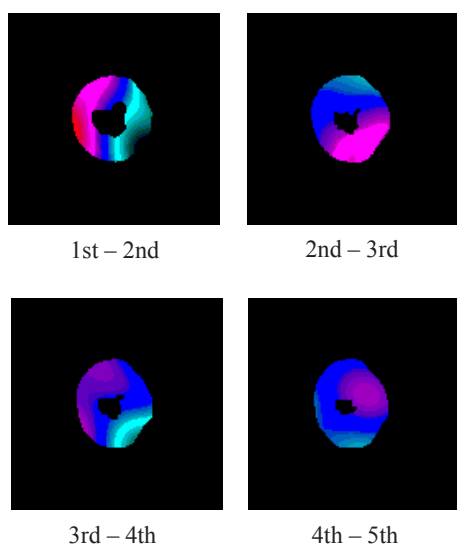
3rd – 4th   4th – 5th

Figure 13: Local map deformation of the myocardium

This kind of results are very interesting for radiologists, extracting from them interesting parameters, like torsion, shearing, longitudinal and radial displacements. This still to be studied with them in order to exactly answer to their expectations.

Moreover, we are currently working on a 3D+T model of the heart, in order to estimate parameters on the whole muscle and not to be limited to 2D+T data.

6   An Information and image processing theory

At last, one of our next goal is to adopt the point of view of EPI in model of active contours. Indeed, these models are the center of our work, and it would be very interesting to show that this image processing tool may guarantee the better uncertainty/inaccuracy compromise all along the detection scheme.

Moreover, in order to quantify this particular compromise during the diffusion process, it would be interesting to develop an entropy-based parameter taking into account the estimation of the validity of the enhanced data by using Fisher Information.

The integration of informational approach in image processing and particularly in medical applications, is an original solution to minimize and quantify the loss of information during a process. Recently, PetitJean and *al* [3] propose such an approach to develop a study of tagged cardiac MR images by a variational non rigid image registration. The used of theoretical methods and the obtained results, show the subjacent unifying potential of such approaches and encourage us to continue our investigations.

References

[1] L. Alvarez and J. Morel. Image selective smoothing and edge detection by nonlinear diffusion. *SIAM Journal of Numerical Analysis*, 29(3):845–866, 1992.

[2] A. Amini, Y. Chen, M. Elayyadi, and P. Radeva. Tag surface reconstruction and tracking of myocardial beads form spamm-mri with parametric b-spline surfaces. *IEEE Transactions on Medical Imaging*, 20:94–103, 2001.

[3] F. Prêteux Ph. Cluzel Ph. Grenier C. Petitjean, N. Rougon. A non rigid registration approach for measuring myocardial contraction in tagged mri using exclusive f-information. In *Proceedings International Conference on Image and Signal Processing (ICISP'2003), Agadir, Morocco*, 25-27 June 2003.

[4] F. Catte, T. Coll, P. Lions, and J. Morel. Image selective smoothing and edge detection by nonlinear diffusion. *SIAM Journal of Applied Mathematics*, 29(1):182–193, 1992.

[5] V. Courboulay, M. Ménard, M. Eboueya, and P. Courtellemont. Une nouvelle approche du filtrage linéaire optimal dans le cadre de l'information physique extrême. In *RFIA 2002*, pages 897–905, Janvier 2002.

[6] J. Declerck, J. Feldmar, and N. Ayache. Definition of a four-dimensional continuous planispheric transformation for the tracking and the analysis of left-

ventricle motion. *Medical Images Analysis*, 2:197–213, 1998.

[7] T. Denney Jr. Estimation and detection of myocardial tags in mr images without user-defined myocardial contours. *IEEE Transactions on Medical Imaging*, 18(4):330–344, 1999.

[8] B.R. Frieden. *Physics from Fisher Information*. Cambridge University Press, 1998.

[9] M. Guttman, E. Zerhouni, and E. McVeigh. Analysis of cardiac function from mr images. *IEEE Computer Graphics and Applications*, 17(1):30–38, 1997.

[10] I. Haber, D.N. Metaxas, and L. Axel. Three-dimensional motion reconstruction and analysis of the right ventricle using tagged mri. *Medical Image analysis*, 4:335–355, 2000.

[11] L. Hermand, A. Histace, and C. Cavaro-Ménard. Analyses d'images irm cardiaques marquées. In *13ème Congrès Francophone AFRIF-AFIA de Reconnaissance des Formes et d'Intelligence Artificielle (RFIA)*, volume 2, page 443, 2002.

[12] A. Histace, C. Cavaro-Ménard, and B. Vigouroux. Tagged cardiac mri : Detection of myocardial boudaries by texture analysis. In *ICIP 2003 Papier Accepté*, 2003.

[13] W.S. Kerwin and J.L. Prince. Cardiac material markers from tagged mr images. *Medical Image Analysis*, 2:339–353, 1998.

[14] J.J. Koenderick. The structure of images. *Biol. Cybern.*, 50:363–370, 1984.

[15] P. Komprobst, R. Deriche, and G. Aubert. Image coupling, restoration and enhancement via pde's. In *International Conference on Image Processing*, volume 2, pages 458–461, October 1997.

[16] D. Kraitchman, A. Young, C. Chang, and L. Axel. Semi-automatic tracking of myocardial motion in mr tagged images. *IEEE Transactions on Medical Imaging*, 14(3):422–433, 1995.

[17] T. Lindeberg. *Scale-Space Theory in Computer Vision*. Pays-Bas, 1994.

[18] P. Perona and J. Malick. Scale-space and edge detection using anistropic diffusion. *IEEE Transcations on Pattern Analysis and Machine Intelligence*, 12(7):629–639, 1990.

[19] P. Radeva, A. Amini, and J. Huang. Deformable b-solids and implicit snakes for 3d localization and tracking of spamm mri data. *Computer Vision and Image Understanding*, 66:163–178, 1997.

[20] A. Rao and R.C. Jain. Computerized flow field analysis : Oriented texture fields. *Transactions on pattern analysis and machine intelligence*, 14(7), 1992.

[21] A.R. Rao. *A taxonomy for Texture Description and Identification*. Springer-Verlag, 1990.

[22] N. Reichek. Mri myocardial tagging. *Journal of Magnetic Resonance Imaging*, 10:609–616, 1999.

[23] N. Rougon and F. Prêteux. Geometric Maxwell equations and the structure of diffusive scale-spaces. In *Proceedings SPIE Conference on Morphological Image Processing and Random Image Modeling*, volume 2528, pages 151–165, 1995.

[24] O. Baylou P. Borda M. Terebes, R. Lavialle. Mixed anisotropic diffusion. In *Pattern Recognition, Proceedings. 16th International Conference on*, volume 3, pages 1051–4651, 2002.

[25] B. Tremblais, B. Augereau, and M. Leard. Multiscale approach for the extraction of vessels. In *Proc. of SPIE Medical Imaging*, volume 5032, pages 1331–1345, 2003.

[26] S. Urayama, T. Matsuda, N. Sugimoto, S. Mizuta, N. Yamada, and C. Uyama. Detailed motion analysis of the left ventricular myocardium using an mr tagging method with a dense grid. *Magnetic Resonance in Medicine*, 44(73-82), 2000.

[27] J. Weickert. Multiscale texture enhancement. In *CAIP'95*, pages 230–237, 1995.

[28] A.P. Witkin. Scale space filtering. In *Int. Joint. Conf. On Artificial Intelligence*, pages 1019–1023, 1983.

[29] A. Young. Model tags : direct three-dimensional tracking of heart wall motion from tagged mr images. *Medical Image Analysis*, 3(4):361–372, 1999.

[30] E. Zerhouni, D. Parish, W. Rogers, A. Yang, and E. Shapiro. Human heart : tagging with mr imaging - a method for noninvasive assessment of myocardial motion. *Radiology*, 169(1):59–63, 1988.

[31] S. Zhang, M. Douglas, L. Yaroslavsky, R. Summers, V. Dilsizian, L. Fananapazir, and S. Bacharach. A fourier based algorithm for tracking spamm tags in gated magnetic resonance cardiac images. *Medical Physics*, 32(8):1359–1369, 1996.